An introduction to modelling flower primordium initiation

Christophe Godin, Eugenio Azpeitia, Etienne Farcot

An introduction to modelling flower primordium initiation

Christophe Godin[1] , Eugenio Azpeitia [2] , Etienne Farcot [3]

December 17, 2015

[1]Inria, Virtual Plants Inria-Cirad-Inra team, 34095 Montpellier Cedex 5, France, France.
[2]Inria, Virtual Plants Inria-Cirad-Inra team, 34095 Montpellier Cedex 5, France, France.
[3]School of Mathematical Sciences, The University of Nottingham, University Park, Nottingham, NG7 2RD

Abstract

In this chapter we present models of processes involved in the initiation and development of a flower. In the first section, we briefly present models of hormonal transport. We focus on two key aspects of flower development, namely the initiation, due to the periodic local accumulation of auxin (a plant hormone) near at the plant apex, and the genetic regulation of its development. In the first section, we described the main assumptions about auxin transport that have been proposed and tested in the literature. We show how the use of models make it possible to test assumptions expressed in terms of local cell-to-cell interaction rules and to check if they lead to patterning in the growing tissue consistent with observation.

Then, we investigated gene regulatory networks that controls the initial steps of flower development and differentiation. In a simplified form, this network contains a dozen of actors interacting with each other in space and time. The understanding of such a complex system here also requires a modeling approach in order to quantify these interactions and analyze their properties. We briefly present the two main formalisms that are used to model GRN: the Boolean and the ODE formalisms. We illustrate on a sub-module of the flower GRN both types of models and discuss their main advantages and drawbacks. We show how manipulations of the network models can be used to make predictions corresponding to possible biological manipulations of the GRN (e.g. loss-of-function mutants).

Throughout the chapter, we highlight specific mathematical topics of particular interest to the development of the ideas developed in the different sections in separated boxes (called Math-boxes). The reading of these boxes is relatively independent of the main text.

Keywords: Developmental models, auxin transport, gene regulatory network, flower initiation, dynamical systems, boolean networks, ordinary differential equations, meristem.

Chapter 1

Making a flower primordium at the tip of a plant stem: a modeling perspective

Contents

1.1 Introduction

A major current challenge in developmental biology is to link gene regulation with shape development. In the last two decades, the spectacular progresses of molecular biology and live imaging have made it possible and to observe animal or plant development in vivo with unprecedented resolution in both space and time. As a consequence, a wealth of new and key data is now available on the various facets of growth: gene expression patterns, geometry of tissue at cell resolution, physical properties of tissues and hormone concentrations, etc.

In the chapter, we will focus on plant development and in particular on the organ that produces all the other plant organs: the apical meristem. Apical meristems consist of small domes of cells located at the tip of each axis and containing undifferentiated cells. Two main types of meristem are usually distinguished, the shoot and the root apical meristems depending on whether they are at the tip of shoot axes or root axes. In this chapter, we will focus our attention to shoot apical meristems (SAMs).

Stem cells at the summit of the SAM slowly divide and provide cells to the surrounding peripheral region, where they proliferate rapidly and differentiate into leaf or flower primordia. Part of these cells give rise to other meristems in a recursive manner, which makes it possible for the plant to build up branching systems (Figure 1.1, see also Chapter 3 which provides a detailed biological account of flower formation).

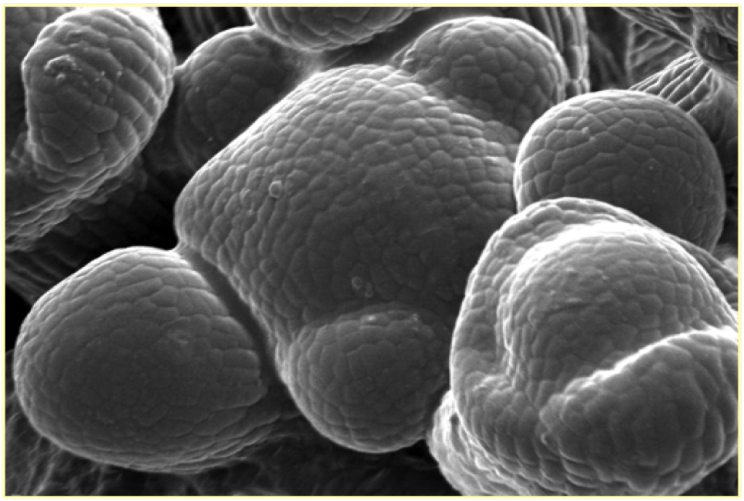

Figure 1.1: Shoot apical meristem of Arabidopsis thaliana (Photo: Jan Traas). At the tip of the Shoot Apical Meristem (SAM), a dome-like population of stem cells proliferates. Organs (here flower primordia) are initiated one after the other at the periphery of this central region, in a spiral pattern where each organ forms an angle of 137° approximately with the previous one. At the bottom right of the picture, a young flower bud is developing and starts itself to produce new lateral organs (here the sepals)

Our aim in this chapter is twofold. We first want to introduce some of the key processes that participate to the functioning and growth of the shoot apical meristem and how they are quantified and modeled. To be focused, we chose to draw our attention to the very moment when an organ is created and a form emerges at the flank of the meristem dome. We shall investigate this morphogenetic event upstream of primordium

initiation, where hormonal signals specify the location of the future primordium, and downstream of organ initiation, where molecular cascades regulating flower development are triggered. Importantly, our second aim in this chapter is to introduce the researchers not familiar with the modeling background used to describe these processes with the mathematical and computational language in a very progressive though precise way. Overall, our aim is to show how models can be used to better to decipher the complexity of the observed phenomena and how they make it possible to deduce facts that can be tested against actual observations.

1.2 Specifying growth points on meristem domes

After initiation at the SAM, the young flower primordium develops as a growing dome. This process obviously involves mechanical forces that locally deform the tissue based on variations stresses in cell walls. The question then arises as to what biophysical or biochemical processes locally trigger these profound physical changes, upstream of these deformations.

In the last decades, researchers have identified potential candidates for these factors. In particular, at the shoot apical meristem, one of the earliest events - may be the earliest one - that precedes the initiation of a primordium has been shown to be a local accumulation of the plant hormone auxin [RMK00]. This accumulation is supposed to induce a cascade of biochemical and biophysical events that locally leads to the outgrowth of a primordium. Therefore two major questions need be understood from a morphogenetic point of view: i) what drives the accumulation of auxin in meristems at precise positions ii) How does the chemical auxin signal is translated into mechanical instructions that lead to primordium outgrowth ?

The latter question is the subject of active research and debates at the moment [HHJ$^+$08, PBLG$^+$11, BP13, SAB$^+$14, BKJ14, BCA$^+$15]. The general idea is that auxin would decrease the rigidity of the cell walls where it accumulates, which in turn would create a bulge in the tissue at the corresponding position as discussed in the previous section. We will not enter further in the description of this molecular mechanisms here.

The former question arises at a wider scale in the plant. Auxin is known to be transported over long distances and the mechanisms that drive this transport have been studied for decades in different tissues since the pioneering work of Sachs, [Sac72]. Interestingly, to achieve differential accumulation of the hormone in different places, this transport process needs be very dynamic and thoroughly coordinated at level of the whole population of cells. As the cells can only interact locally with their immediate neighbors in the tissue, this coordination must therefore essentially be an emergent property of this complex cell-to-cell interaction network. To better understand this phenomenon, researchers have attempted to model the emerging organization of the auxin transport through the cell network based on different hypothetical cell-to-cell interaction rules. We are going in the sequel to describe the principles of these models.

1.2.1 Auxin import and export in cells

Auxin refers to a group of small molecules, the most current example of which being the Indole Acetic Acid (IAA), that can be transported through cells in plant tissues. This transport is mainly due to the presence in cells of membrane carriers of efflux or influx that make it possible for auxin to pass through cell membranes, see [KJ10, RSP14] for general presentations of auxin transport models in plants.

Let us first have a closer look at the general mechanism behind the transport of auxin molecules through the cell membranes and walls. The principle of this transport has been proposed in the 70's by [RS74, Rav75], and is known as the Chemiosmotic theory, Figure 1.2. In brief, the idea is that auxin exists in two forms in plant tissues, a neutral protonated form $IAAH$ and an anionic form IAA^-. The protonated form can diffuse freely across the cell wall while the anionic form cannot. The relative proportion of these two forms depends on the medium pH e.g. [KB06]). In the cytoplasm, whose pH is neutral ($pH7.0$), auxin is mostly in its anionic form IAA^- whereas in the

acidic apoplast compartment ($pH5.5$) the neutral form exists in a much higher proportion. Therefore, in the absence of other processes, auxin can passively diffuse from the apoplastic compartment inside the cells but, then gets trapped in its anionic form in the cytoplasm. To get out of the cell to the apoplast, the anionic form needs specific molecular carriers.

This is done by membrane transporter proteins PIN1 of the PINFORMED family. The PIN1 proteins are putative efflux carriers, i.e. they actively contribute to get auxin out of the cell to the intercellular compartment (the apoplast). PIN1 proteins are polarly located in the cell membranes (i.e. at a given moment in time, they are located on a particular side of the cell). Another family of transporters, the AUX/LAX proteins, contribute to the transport of auxin from the apoplast into the cell cytoplasm (AUX/LAX proteins are active influx carriers). They are not polarized in the cell and usually cover uniformly the surfaces of the cell membranes.

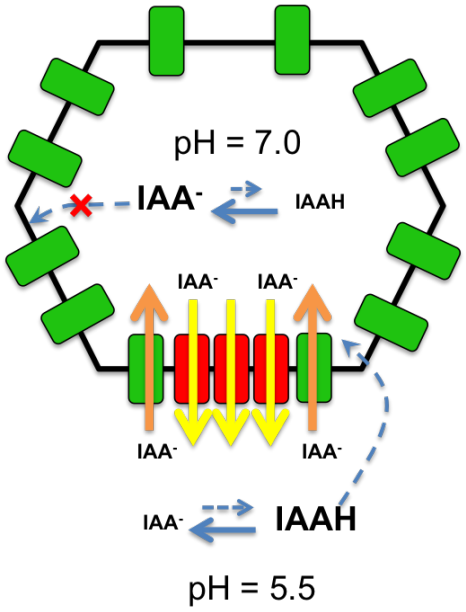

Figure 1.2: **auxin transport across cell plasma membranes**. In the cytoplasm with neutral pH, the anionic form largely dominates and can get out of the cell only via efflux carriers (e.g. PIN1 proteins in red). In the apoplastic compartment, the neutral form can diffuse freely to the cytoplasm. Additional transport of the anionic form from the apoplast to the cytoplasm requires an influx carrier (e.g AUX proteins in green).

1.2.2 Auxin flows in the meristem

Now let us consider the question of auxin transport at a larger scale, over an organ or a particular tissue. Such a coherent long distance transport is due to the possibility for the cells to coordinate their activities and orient consistently their PIN1 polarities. In this way, the cells create pathways through the tissue in which auxin is transported from place to place. In the shoot apical meristem, this dynamic network of PIN1 pumps is coordinated in such a way that it leads periodically to the creation of small auxin patches in the L1 layer close to the tip [RPS$^+$03].

To understand how such a system can work at the level of cell populations, it is useful to model quantitatively this dynamic transport process. Let us start by modeling auxin transport for a fixed configuration of the PIN polarity within the cells. The description of the transport then consists of quantifying the conservation of auxin molecules at any point of the tissue. Note that for sake of simplicity, we neglect here the action of the influx transporters of the AUX/LAX family (however, this role may be important to maintain a certain level of robustness in the patterning, see [KB06, BGB$^+$08]).

Let us formalize this. Consider a meristem tissue made up of a collection of cells i whose states are defined by a concentration of auxin a_i ($mol.m^{-3}$) and a volume v_i. If there exist PIN proteins polarized in cell i toward neighboring cell n, then we consider that auxin can be actively exported from cell i to cell n. In this transport network, processes that may affect the auxin concentration a_i of each cell i are of three different types:

- *Transport*: Auxin molecules may move within the network of cells. It is usually considered that this movement has two potential sources (chemiosmotic model):
  - *passive transport*: due to thermal noise, auxin molecules may randomly move from cell to cell.
  - *active transport*: auxin molecules can be exported outside of the cell by membrane transporters.
- *Synthesis*: auxin may be synthesized locally cells.
- *Degradation*: a percentage of the auxin molecules may be regularly degraded (or inactivated) within the cell itself.

The variation of auxin concentration in each cell can be modeled by quantifying these processes and combining their effect in an equation reflecting the conservation of auxin molecules in the network of cells through space and time. Fluxes in the tissue will make it possible to quantify the net auxin movement between cells (see Math-Box:Fluxes and cell concentrations). The rate of change of a_i is therefore defined by:

$$\frac{\partial a_i}{\partial t} = -\frac{1}{v_i} \sum_{n \in N_i} s_{i,n} \phi_{i \to n} - \delta_a a_i + \sigma_a, \tag{1.1}$$

where $s_{i,n}\phi_{i \to n}$ is the net flux of auxin from cell i to cell n through the interface surface $s_{i,n}$, σ_a ($mol.m^{-3}.s^{-1}$) is a constant that describes the rate at which auxin is produced in cells and δ_a (s^{-1}) defines the rate of auxin degradation. Both constants are considered here independent of the cell state (no subscript i).

Relation between fluxes and concentrations of molecules in cells

To compute the net amount of of molecules that enter the cell during a certain time, one needs to consider the *net flux* of molecules through the different faces of the cell.
Let us consider two compartments A and B separated by a membrane of surface $s_{A,B}$ (m^2). We define the *flux density* $\phi_{A\to B}$ $(mol.m^{-2}.s^{-1})$ through the surface $s_{A,B}$ as the net number of molecules that cross the membrane from compartment A to compartment B per unit surface and per unit time (note that direction A to B is meaningful here). A positive flux density from A to B means that molecules are transferred from A to B. Reciprocally, a negative flux means that molecules are transferred from B to A. The total flux through surface $s_{A,B}$ separating compartment A and B is then defined by $s_{A,B}\phi_{A\to B}$.
Based on fluxes, it is easy to compute the net flux Φ_i of molecules that enter a cell i per time unit. In a tissue, consider the membrane that separates a cell i from one of its neighboring cells n, crossed by a flux density $\phi_{n\to i}$. If $s_{i,n}$ denotes the surface of this membrane, then the net flux that crosses the surface $s_{i,n}$ per time unit is $(mol.s^{-1})$:

$$\Phi_{n\to i} = s_{i,n}\phi_{n\to i}, \tag{1.2}$$

and by summing up on all the interfaces of cell i with other cells n, we get the total net amount of molecules that entered cell i during a unit time:

$$\begin{aligned}\Phi_i &= \sum_{n\in N_i} s_{i,n}\phi_{n\to i} \\ &= -\sum_{n\in N_i} s_{i,n}\phi_{i\to n} = -\sum_{n\in N_i}\Phi_{i\to n}.\end{aligned} \tag{1.3}$$

Consequently, if we assume that molecules can only remain, move in or out of cells to their neihgbours, the concentration a_i of a particular molecule in cell i of volume v_i will change at rate:

$$\begin{aligned}\frac{\partial a_i}{\partial t} &= \frac{\Phi_i}{v_i} \\ &= -\frac{1}{v_i}\sum_{n\in N_i} s_{i,n}\phi_{i\to n}.\end{aligned} \tag{1.4}$$

By decomposing the net total flux $\Phi_{i\to n}$ through the membrane between i and n in a net flux due to diffusion $\Phi^D_{i\to n}$ and a net flux due to active transport $\Phi^A_{i\to n}$, we get:

$$\phi_{i\to n} = \phi^D_{i\to n} + \phi^A_{i\to n}, \tag{1.5}$$

and by replacing $\phi_{i\to n}$ in equation 1.1, it comes:

$$\frac{\partial a_i}{\partial t} = -\frac{1}{v_i}\sum_{n\in N_i} s_{i,n}\phi^D_{i\to n} - \gamma_a\sum_{n\in N_i} s_{i,n}\phi^A_{i\to n} - \delta_a a_i + \sigma_a. \tag{1.6}$$

Let us now make explicit in this equation the diffusion and the active transport terms. The density of flux due to diffusion between two compartments is classically assumed to be proportional to the difference of concentrations between these compartments (a particular case of Fick's First Law) :

$$\phi^D_{i\to n} = \gamma_D \left(a_i - a_n\right), \tag{1.7}$$

where γ_D is the constant of permeability reflecting the capability of auxin to move across the membrane ($m.s^{-1}$).

The net density of flux due to active transport depends on the distribution of carrier proteins that one can find in membranes on both sides of a given wall between two cells i and n. A model of this type was originally proposed by Mitchison [Mit80, Mit81] and makes it possible to express the density of flux through the wall $s_{i,j}$ as a function of the auxin concentration in the neighboring cells:

$$\phi^A_{i\to n} = \gamma_A \left(a_i p_{i,n} - a_n p_{n,i}\right) \tag{1.8}$$

where γ_A ($m^3.mol^{-1}.s^{-1}$) characterizes the transport efficiency of the PIN proteins and $p_{i,n}$ ($mol.m^{-2}$) is the surfacic concentration of PIN proteins in the membrane of cell i facing cell n facilitating transport from cell i to cell n.

The equation can be interpreted as if each single carrier protein PIN in the wall would transport $\gamma_A a_i$ molecules of auxin. Since there are $p_{i,n}$ PIN molecules per unit of surface in the wall, each unit of surface exports $\gamma_A a_i p_{i,n}$ molecules [FMI05]. Equation 1.1 thus becomes:

$$\frac{\partial a_i}{\partial t} = -\frac{\gamma_D}{v_i}\sum_{n\in N_i} s_{i,n}\left(a_i - a_n\right) - \frac{\gamma_A}{v_i}\sum_{n\in N_i} s_{i,n}\left(a_i p_{i,n} - a_n p_{n,i}\right) - \delta_a a_i + \sigma_a, \tag{1.9}$$

showing on the right member respectively from left to right a term of diffusion, a term of active transport, a term of auxin decay and a term of auxin synthesis.

Different variants of this model have been used in the literature to simulate auxin flows in the meristem. A first application was to estimate auxin distribution in meristems based on observed and precise maps of the polar PIN transporters in cells [BdRBCL$^+$06]. Indeed, while auxin concentrations are extremely difficult to measure at cell resolution (in a cell or a small group of cells), the presence of PIN transporters in cell membrane can be observed with good accuracy using confocal microscopy. The idea was then to estimate the auxin distributions in the observed meristem at a given date from the observed distribution of PIN proteins in confocal images by simulating the transport of auxin in the observed networks of PIN "efflux pumps". This made it possible to confirm that auxin was indeed accumulating and to predict that, according to the observed distribution of transporters, auxin should accumulate in the central zone of the meristem [BdRBCL$^+$06]. This prediction has been confirmed experimentally several years after with the use of a new auxin sensor [VBF$^+$11].

Other applications have used variants of this transport model to assess the plausibility of different assumptions concerning the origin of the observed PIN polarity. Some of these variants integrate a more detailed description of chemiosmotic model. An apoplast compartment for instance is added to the previous model and protonated and non-protonated versions of auxin are distinguished, e.g. [SSJ09]. Other refinement include the introduction of AUX/LAX influx carriers, e.g. [Kra04], a representation of the trafficking inside the cell between PIN1 molecules embedded in the plasma membrane and a pool of "free" molecules available in the cytoplasm, e.g. [JHS+06, WKVB+10].

In the growing tissue, the PIN distributions are very dynamic. Their allocation to different membranes of a particular cell can change in an hour, thus leading to a very plastic and dynamic configuration of the auxin transport network in the meristem. Here again the processes that drive this dynamic reconfiguration of the network is poorly understood. However, several hypothesizes have been proposed to explain the various self-organized patterns of the PIN molecules observed in various plant tissues.

1.2.3 Allocating PIN to cell membranes

While the regulation of PIN polarization is a key determinant of primordium formation, little is known about the underlying biochemical or physical processes. Research on the plausible detailed molecular mechanisms is currently in progress, e.g. [HHK+10, WKVB+10]. However, at a coarser scale, different hypotheses have been proposed to interpret the dynamics of PIN carriers in different tissues and their self-organizing ability. All these mechanisms rely on a positive feedback loop between the auxin concentration or the auxin flux and the PIN dynamic allocation process.

***Concentration-based* hypothesis** It has been observed in the meristem that auxin accumulates in small spots close to the tip. Based on GFP labelling of PIN carriers, a closer inspection of the distribution of the PIN polarities in the corresponding cells reveals that in these cells, PIN tend to accumulate in the cell on the membrane facing the center of the spot. As the auxin signal appears to be maximal at the center of the spot, it has been suggested that the PIN carriers could actually be allocated to the cell membranes in proportion of the amount of auxin contained in the corresponding adjacent cells [SGM+06, JHS+06], Figure 1.3.A. This behavior can be captured for example by the following polarity law [SGM+06]:

$$p_{i,n} = \frac{s_{i,j} b^{a_j}}{Z} p_i, \tag{1.10}$$

where p_i is the total concentration of PIN molecules in cell i, $s_{i,j}$ is the surface separating cell i and j, b is a parameter controlling the intensity of the influence of cell j on cell i and a_j is the auxin concentration of cell j. Z is a normalizing coefficient, corresponding to the fact that altogether in a given cell, all the $p_{i,n}$ must sum up to p_i:

$$Z = \sum_j s_{i,j} b^{a_j}, \tag{1.11}$$

In the concentration-based hypothesis, auxin peaks (if any) are reinforced by their neighboring cells that orient their PIN pumps towards the peak, against the auxin gradient. Similarly to Turing reaction-diffusion systems, this system is able to spontaneously

generate spatial patterns [SGM+06, JHS+06, SSJ09], Figure 1.3.B. A tissue with an initial uniform auxin distribution and subject to local random fluctuations will break this spatial symmetry and evolve toward a stable state where the system self-organizes with spatial motifs corresponding to periodic accumulations of auxin concentration throughout the tissue (see Figure 1.3.B).

***Flux-based* hypothesis** The concentration-based hypothesis was introduced rather recently as a means to explain the auxin patterns in the SAM. However, in the 70s, another feedback mechanism was proposed by T. Sachs to explain the development of vascular vessels during leaf development [Sac69, Sac00]. Sachs suggested that a positive feedback in the tissue reinforces and stabilizes existing auxin fluxes. This mechanism would be able to reconfigure the transport network dynamically in case of obstacles or wounds and would be responsible for the establisment of veins patterns in leaves. In 1980, Mitchison used quantitative models to show using computer simulations that if the feedback of the flux on the cell export in the direction of the flux is strong enough, the system can indeed create canals [Mit80, Mit81]. This so called "canalization" system is now recognized as a fairly plausible mechanism of vein formation [RFL+05, SMFB06, BRB+11], Figure 1.3.C. This canalization system was later revisited by Roland-Lagand [RLP05] who suggested that the feedback could be mediated by the PIN1 proteins in plant tissues and by [FMI05] who explored further the mathematical properties of this dynamical system. In Math-Box *Flux-Based Transport: Local properties*, we illustrate the type of mathematical analysis that can be made of such a model and the insights that may be gained on the system by mathematical derivation.

Formally, it is assumed that the concentration of PIN proteins $p_{i,n}$ in cell i transporting auxin to cell n changes due to i) insertion of PIN proteins in the membrane induced by the flux ii) a background insertion and iii) removal of PIN1 from the membrane. The balance between these processes can be captured by the equation:

$$\frac{\partial p_{i,n}}{\partial t} = F(\phi_{i\to n}) + \alpha_p - \beta_p p_{i,j}, \tag{1.12}$$

where

$$\begin{aligned} F(\phi_{i\to n}) &> 0 \qquad \text{if} \quad \phi_{i\to n} > 0, \\ &= 0 \qquad \text{if} \quad \phi_{i\to n} \leq 0. \end{aligned} \tag{1.13}$$

F is a function that expresses how the flux of auxin through a particular membrane feeds back on the PIN1 allocation to that membrane. Feugier et al. showed that only super-linear functions (i.e. function that grow faster than the identity function) induce canals. For example, a quadratic feedback function ($F(x) = \gamma_p x^2$) would lead to:

$$\frac{\partial p_{i,n}}{\partial t} = \gamma_p \phi_{i\to n}^2 + \alpha_p - \beta_p p_{i,j},$$

The feedback generated by superlinear functions is such that, when a cell receives enough auxin, it switches to a mode where a large efflux through one wall only is preferred to smaller effluxes through many walls simultaneously (see [Feu06]). This corresponds to a bifurcation in the dynamical system that switches the system from a non-canalized to a canalized mode when auxin fluxes are sufficient (see Math-Box Dynamical Systems in the next section), see Figure 1.3.D. At the tissue level, superlinear

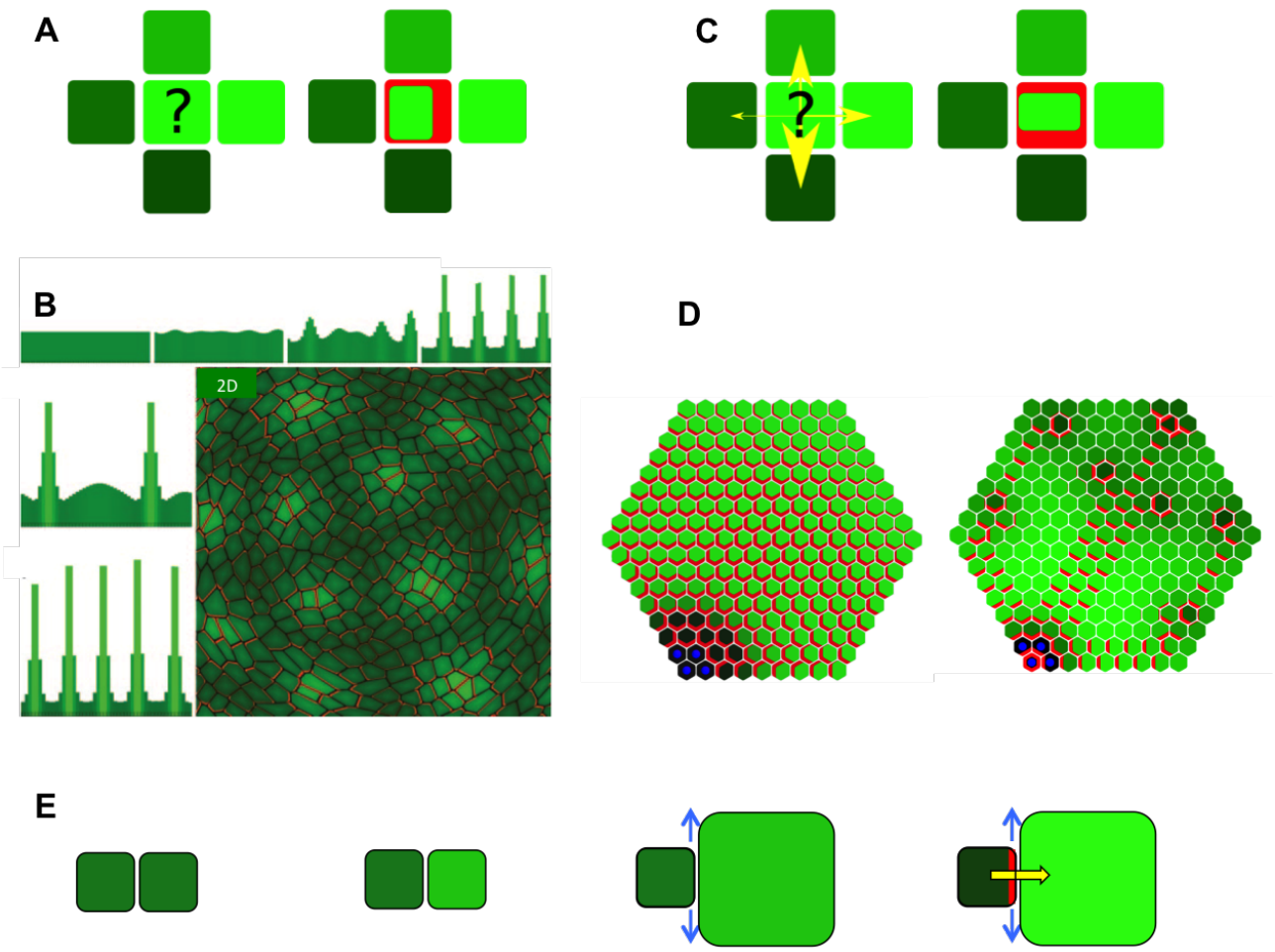

Figure 1.3: Different hypotheses for the dynamic allocation of PIN molecules to membranes. A. Concentration based hypothesis. Neighboring cells of a cell i are assumed to have different concentrations of auxin (left: bright green is high concentration, dark green is low, figures A/C/D reproduced from [SLC+08]). Concentration-based rule indicates that PINs should be allocated in proportion of the auxin contained in each neighbor (right) B. Turing-like patterns emerging spontaneously from the concentration-based (Figure reproduced from [SGM+06]): emergence of auxin peaks due to noise perturbation of an initially homogeneous concentration. Different wave length can be acheived depending on the odel parameters (below left panels). Spatial periodicity generated by the system in 2D (Bottom right panel). C. Flux-Based hypothesis. Yellow arrows indicate the intensity of the auxin fluxes through the different walls (bigger arrow for higher flux). Flux-based rule allocates more PINs to membranes crossed by a higher flux (right). D. Patterns resulting from flux-based rule: a sink (in blue) attracks auxin. Two regimes can appear depending on the strength of the feedback function F: linear function: no-canals are formed (left) super-linear function: canals appear (right) E. Stress-based hypothesis. Starting from two cells having similar amount of auxin (left), and assuming that one of the two cells gets higher auxin level (right cell in brighter green in central left panel), the right cell is thus instructed to grow faster (central right panel), which puts the cell wall of the left cell in tension and triggers more allocation of PINs to this wall according to the stress-based rule (right panel). Note that this mechanism amplifies the concentration differences and thus implements a concentration-based rule.

functions thus induce the formation of canals that are believed to be at the origin of vascular tissues in plants (Figure 1.3.D).

Flux-Based Transport: Local properties

To ease the analysis and get first insight in the model, the system can be simplified and studied locally. For this, a single cell i is considered and auxin and PIN in its immediate neighbors are assumed to be negligible ($\forall n \in N_i, a_n = 0$ and $p_{n,i} = 0$), though we consider the interface with these neighbors and the distribution of PIN towards them. In this "isolated" context the variations of auxin, Eq. (1.9), takes the simpler form:

$$\frac{\partial a_i}{\partial t} = -\left(\frac{\gamma_D}{v_i}\sum_{n\in N_i} s_{i,n}\right) a_i - \frac{\gamma_A}{v_i}\sum_{n\in N_i} s_{i,n} a_i p_{i,n} - \delta_a a_i + \sigma_a,$$

which makes it possible to compute the steady state level of auxin ($\frac{\partial a_i}{\partial t} = 0$) in terms of PIN concentration at the different interfaces with neighbors, using the short-hand notation $\delta = \delta_a + \frac{\gamma_D}{v_i}\sum_{n\in N_i} s_{i,n}$.:

$$a_i = \frac{\sigma_a}{\delta + \frac{\gamma_A}{v_i}\sum_{n\in N_i} s_{i,n} p_{i,n}}.$$

To determine a_i one therefore needs to estimate the values of $p_{i,n}$ for each $n \in N_i$ at the steady state. In the same single-cell context, the equation (1.12) for PIN variables gives, for each $n \in N_i$:

$$p_{i,n} = \frac{1}{\beta_p} F(p_{i,n} a_i) + \frac{\alpha_p}{\beta_p} = \frac{1}{\beta_p} F\left(\frac{\sigma_a p_{i,n}}{\delta + \frac{\gamma_A}{v_i}\sum_{l\in N_i} s_{i,l} p_{i,l}}\right) + \frac{\alpha_p}{\beta_p}.$$

Since a_i is entirely determined by the $p_{i,n}$ (see the above expression of a_i at equilibrium), the "isolated" steady state is given by solving the equation above for each $n \in N_i$. Interestingly, one particular solution where all $p_{i,n}$ are equal ($p_{i,n} = p$ for every $n \in N_i$), corresponds to a non-polarized cell. This solution is given by a fixed point equation:

$$p = G(p)$$

with

$$G(p) = \frac{1}{\beta_p} F\left(\frac{\sigma_a p}{\delta + p\frac{\gamma_A}{v_i}\sum_{l\in N_i} s_{i,l}}\right) + \frac{\alpha_p}{\beta_p}$$

This analysis makes it possible to discuss symmetry issues, key to the study of cell polarization. For example, depending on the exact form of the function F, there can be other solutions, where the $p_{i,n}$ are not all identical. These solutions are less symmetric than the former and correspond to cell polarization. In general, both symmetric and asymmetric solutions co-exist, but only one of them might be stable (cf. frame 'Dynamical Systems' in the next section), depending on

... *continued :* Flux-Based Transport: Local properties

parameter values, i.e. there exists critical parameter values at which a bifurcation occurs.
The precise conditions in which this breaking of symmetry occurs, i.e. for which form of function F and at which parameter values, are not fully known and constitute a research topic for mathematical modellers.
Another issue related to the symmetry of the problem is due to the fact that since all $p_{i,n}$ are given by the exact same equation, any 'polar' solution where PINs are not all identical is geometrically not completely determinate. For instance, it is not possible to distinguish between a solution where $p_{i,1}$ is low on a wall and $p_{i,2}$ high on another wall and the reverse situation. This ambiguity is in fact resolved by considering the problem at a larger scale, discussed in the next frame.

***Stress-based* hypothesis** Recently, a strong correlation between the positioning of PIN molecules and microtubule orientation in cell membranes has been observed in apical meristems [HHK+10]. This study shows that microtubules are preferentially oriented parallel to PIN1 positioning in cell membranes. However, the orientation of microtubules themselves appears to be correlated to mechanical stresses in cell walls [HHJ+08]. This therefore suggests that the polarized presence of PIN1 in cells could be a consequence of the local stress variations in cell walls. To interpret these observations, a model coupling PIN1 allocation to mechanical stresses has been introduced [HHK+10]. In a cell i, this model relates the amount of PIN1 allocated to a membrane facing a neighboring cell n to the amount of stress, $\sigma_{i,n}$, existing in the wall between i and n in a proportional manner:

$$p_{i,n} = \lambda_1 \frac{\sigma_{i,n}^m}{Z} p_i, \tag{1.14}$$

where p_i is the total concentration of PIN molecules in cell i, m is a constant parameter controlling the relative intensity of the stress feedback in each wall on PIN allocation to walls, a_i is the auxin concentration of cell i, and λ_1 is a constant parameter. Z is a normalizing coefficient, corresponding to the fact that altogether in a given cell, all the $p_{i,n}$ must sum to p_i:

$$Z = 1 + \lambda_1 \sum_n \sigma_{i,n}^m, \tag{1.15}$$

where the 1 in the right-hand side expression is here to avoid the cancellation of the denominator when the cell has no stress in its walls.

The model then assumes that the amount of auxin present in a cell modulates the elastic property of the cell walls: the more auxin, the less rigid the cell walls. This rule is formalized by the following equation relating the elastic modulus E in cell i's walls to the cell's auxin concentration a_i:

$$E(a_i) = E_{min} + \frac{\lambda_2 (E_{min} - E_{max})}{\lambda_2 + a_i^r}, \tag{1.16}$$

where E_{min} and E_{max} are minimal and maximal values of the cell's elastic modulus respectively, λ_2 is a constant parameter and r is a parameter controling the strength of the dependence between the wall elasticity and the cell's auxin concentration.

Hence, if a cell locally gets more auxin than its neighbors (Figure 1.3.E middle left) the rigidity of its wall is decreased and the cell walls tend to elongate (Figure 1.3.E middle right). Walls being rigidly connected between cells, this extension induces and augmentation of stress in the walls of neighboring cells (Figure 1.3.E middle left, blue arrows). Viewed from the neighboring cell, this corresponds to a differential augmentation of stress in its wall, which in turn, leads the neighboring cell to allocate more PIN1 molecules to this wall according to equation 1.14 (Figure 1.3.E right). Interestingly, one can observe that this mechanism is a special case of the concentration-based hypothesis (see above), where additional hypotheses are made about the mechanism by which the neighboring cells allocate more auxin on the side the the cell that contains a higher auxin concentration.

1.2.4 Accumulation of auxin at the meristem surface

These different hypotheses have been used to model the dynamic accumulation of auxin at the tip of SAMs, upstream of organ formation. Based on additional assumptions, they all could be used successfully to reproduce spiral phyllotaxis patterns observed in real Arabidopsis meristems. The concentration-based hypothesis was first shown to be a plausible explanation of phyllotaxis by two teams independently [SGM$^+$06, JHS$^+$06]. In these works, auxin transport is modeled in the L1 layer of cells (outermost layer of cells in the meristem) by assuming that auxin is produced and degraded in every cells and is transported up-the auxin gradient by PIN1 molecules, according to concentration-based rules similar to that of equation 1.10. Both models were implemented and simulated on an artificial growing tissue, including basic rules for cell growth and division. Simulations showed that phyllotactic patterns of different types, both spiral and whorls, could be recapitulated from the dynamic models, based on purely local cell to cell interaction rules (here concentration-based rules for PIN1 allocation to membranes, and auxin transport rules similar to equation 1.9).

The success of these models to reproduce the dynamics of phyllotactic patterns in the growing meristem raised however a new important question. If such a concentration-based process is at work to polarize PIN1 proteins in the L1 layer, it is however believed that veins in plant organs are initiated by canalization processes related to the flux-based hypothesis. This latter view is supported by a considerable amount of experimental observations and models [Sac69, Mit80, RLP05, RFL$^+$05, FI06, SMFB06, WKVB$^+$10]. The picture concerning the dynamic allocation of PIN1 to cell membranes would then be that a concentration-based process would prevail in the L1 layer to explain the periodic accumulation of auxin peaks, while a flux-based process would be involved in other parts of the tissue, where veins are observed. This idea of a combination between different models in different tissues was developed further in Bayer et al. who tried to assemble both processes in a single model. For this, the authors assume that both mechanisms (flux- and concentration-based) can be triggered by a cell. However, the relative importance of each mechanism is controlled by the auxin level of the cell: at low auxin concentration, the PIN allocation process is dominated by the concentration-based mechanism, while at high auxin concentrations, it is dominated

by the flux-based mechanism. In the L1 layer, where levels of auxin are low except in the newly formed primordia, the concentration-based rule therefore dominates in the transport process, leading to regular accumulation of auxin at the periphery of the central zone. In the incipient primordium however, the accumulation of auxin is maximal and triggers the flux-based mechanism while weakening accordingly the action of the concentration-based one (hypothesis of the combined model). Consequently, a flux of auxin is initiated in the initium downwards, towards the inner tissues, and the flux-based mechanism builds up a canal from the auxin source (the initium) to the auxin sink (the inner parts of the tissue). This canal is assumed to initiate the provascular tissues beneath the new organ. Interestingly, this model predicted that, at the moment of initiation, just before switching on the flux-based process, a transient polarization of PIN1 pointing upwards in the inner tissues should be observed. Despite the fact that such transient phenomena are difficult to capture, this prediction could indeed be verified on confocal images of tomato and *Arabidopsis* meristems, [BSM$^+$09].

An alternative approach to this combined model was developed by [SLC$^+$08], based on the idea that a unique model could possibly be active both at the surface of the meristem and in the inner layers. Stoma et al. then tested the possibility that a flux-based mechanism could explain the accumulation of auxin in the L1 layers. They showed that when primordia are considered to be imperfect sinks for auxin, flux-based systems can transport auxin against the auxin gradient. They then showed that such a transport hypothesis can lead to correct phyllotactic patterns and therefore constitute a plausible transport mechanism in the L1 layer as well. Based on this result, they showed that a flux-based system could be both used in the L1 layer and in the inner tissues. However, the authors could not find a unique region in the parameter space where both L1 fluxes against the gradient and canalization in inner tissues would work simultaneously. This defect in the parsimony of the approach was later corrected in [**?**] who showed that parameters of the flux-based model common to the L1 layer (sink-driven patterning) and to the inner layers (source driven patterning) can be selected in order to reproduce both the diffused patterns of PIN polarization in the M1 layer and the strand patterns in the inner layers.

All the models considered so far have their qualities and deficiencies, and account to varying degrees of biological facts. Based on our current knowledge of the transport processes, it is not possible to conclude with certainty in favor of any particular model. In recent years, other related models or variants of the previous models have been introduced, e.g. [WKVB$^+$10, ABdRS$^+$13] and rely on a refined understanding of the molecular processes underlying the transport systems. It is no doubt that a better biological understanding of the molecular and biophysical processes involved in hormone transport at the SAM will eventually make it possible to progress in the modeling of hormone transport at the SAM and to eliminate progressively unrealistic hypotheses. However, these models are complex as their global behavior emerges from local rules of interactions between cells and feedback loops between biochemical or physical variables. Progress on these models will certainly also require a systematic analysis and better understanding of their mathematical and formal properties (steady states, symmetry breaking, bifurcations, network properties, etc.), e.g. [FMI05, PCS$^+$09, WFTG13, vBdBStT13, FY13, FFM15], see also Math-Box *Flux-Based Transport: Global Constraints* below.

Flux-Based Transport: Global Constraints

The distribution of auxin and PIN at steady state is not only determined by the local, intra-cellular dynamics (see previous frame), but also by how the fluxes of auxin combine at the multi-cellular level.
Mathematically, the spatial domain on which auxin transport is studied is a graph $G = (V, E)$, whose node set V represent cells and edges $E \subset V \times V$ represent areas of cell membrane that are at the interface between neighbouring cells.
One important property comes from the fact that

$$\phi_{i\to j} = -\phi_{j\to i}\,,$$

as follows immediately from the definition $\phi_{i\to j} = \gamma_D\,(a_i - a_j) + \gamma_A\,(a_i p_{i,j} - a_j p_{j,i})$.
This properties entails a global constraint: the sum of all fluxes in the tissue must be zero.
Also, from the relation above and the fact that in Equation (1.12) the function F is zero for non-positive flux, it follows that at steady state it is always true that either

$$p_{i,j} = \tfrac{\alpha_P}{\beta_P} \qquad \text{or} \qquad p_{j,i} = \tfrac{\alpha_P}{\beta_P}.$$

Indeed, the steady state equations are, for any $(i, j) \in E$

$$p_{i,j} = \tfrac{1}{\beta_P}\,(F(\phi_{i\to j}) + \alpha_P) \qquad \text{and} \qquad p_{j,i} = \tfrac{1}{\beta_P}\,(F(\phi_{j\to i}) + \alpha_P)\,,$$

where one of $\phi_{i\to j}$, $\phi_{j\to i}$ is non-positive. In other terms, at least one of the two variables $p_{i,j}$, $p_{j,i}$ must be fixed to the value $\frac{\alpha_P}{\beta_P}$, while the other one is either at the same value, or at a higher value (because the function F is non-negative).
This property forces some PIN variables to the low concentration $\frac{\alpha_P}{\beta_P}$. In the previous frame, we have seen that within each cell, solving steady state equations can provide us with the information of "how many" PIN variables take a given values, but not which ones exactly. Now that we are considering the whole tissue, we can see that additional constraints will actually partially resolve this ambiguity.
One can interpret the situation loosely as follows: each edge (i, j) of the graph G can be oriented in the direction of the globally constrained flux, which forces one of the two variables $p_{i,j}$, $p_{j,i}$ to a low value. In addition, the internal flux within each cell determine how many 'high PIN walls' are possible. Every configuration that simultaneously matches the two constraints, one global and one local, is a steady state.

1.3 Modeling the regulation of flower initiation

As we discussed in the previous section, flower primordia are initiated in the SAM due the self-organized accumulation of auxin at the periphery of the SAM central zone. This accumulation locally triggers flower development [RMK00] and a cascade of genetic regulation. In this section, we will describe how such regulatory networks can be modelled and the main mathematical formalisms to achieve models of dynamical systems (see Math-Box *Dynamical systems*).

Dynamical Systems: Definitions

As indicated by the term, a **dynamical system** is a system that evolves in time. This notion can be formalized mathematically in an abstract way, which encompasses all the more specific forms that are used in this chapter.
To describe how a system evolves in time, one needs to have a representation of time, and a representation of the system's state at a given instant. One also needs a transformation rule to describe the effect of time on the system's state. Mathematically, a dynamical system is nothing more than these three elements:
Definition: A dynamical system is a triple (S, T, Φ) where:

- S is a set, very often endowed with a notion of neighborhood or distance, called **state space**.
- T is a set describing time, usually endowed with a notion of order, an addition rule $+$, and an origin 0 which is neutral for addition ($t + 0 = t$).
- Φ is a map $S \times T \to S$ which, given a state $x \in S$ and a time $t \in T$ returns the new state $x' = \Phi(x, t)$ of the system after a duration t if it is in state x at $t = 0$. This **evolution operator**, also called **flow**, must satisfy the following intuitive axioms:
  - $\Phi(x, 0) = x$ for any state $x \in S$.
  - $\Phi\left(\Phi(x, t), t'\right) = \Phi(x, t + t')$ for any $x \in S$ and $t, t' \in T$.

Although the notion of flow covers all examples of dynamical systems that will be seen in these lectures, it is not always used explicitly (see Frames 'Discrete/Contiuous Time'). It is still a very useful concept as it allows to define important notions in a unified way. Such notions include:

- The **trajectory** (sometimes also called **orbit**) of a state x is the set of all past and future states $o(x) = \{\Phi(x, t) \,:\, t \in T\}$.
- A **steady state** is a state that does not change in time: $\Phi(x, t) = x$ for all t. Its trajectory is a single point: $o(x) = \{x\}$.
- A **periodic trajectory** is a trajectory $o(x)$ such that there exists a time $\tau \in T$, called the period, such that $\Phi(y, \tau) = y$ for any point $y \in o(x)$ (including $y = x$). Geometrically, $o(x)$ is a closed loop in state space.

... continued : **Dynamical Systems: Definitions**

- A steady state x (or periodic trajectory $o(x)$) is called **stable** if for every state y close enough to x, the future states $\Phi(y,t)$ become arbitrarily close to $o(x)$ when $t \to \infty$. It is called **unstable** otherwise, i.e. if one can find an y arbitrarily close to x such that $o(x)$ and $\Phi(y,t)$ do not get close in the limit $t \to \infty$.

1.3.1 Expression patterns in the flower meristem

During its development, the flower meristem is divided in regions, which have differential gene expression patterns. There are many genes correlated with the different regions and developmental phases of the flower meristem. However, here we will only cover the main ones, (for a more comprehensive review see Chapter 3 in this book and [Cha12, ABBitCPe+10, LTY09]). Inflorescence meristems produce flower primordia at the axils of cryptic bracts, at points of high auxin concentration ([YWW+13, Cha12]). The auxin peaks are generated in a phyllotactic pattern created by auxin flux, as described above. Then, LEAFY (LFY) and APETALA1 (AP1) expression is established all over the flower meristem ([RAV+98]). LFY and AP1 are important genes for flower development and the establishment of the flower meristem identity, since their mutants have several flower defects, which range from late flowering, flower reversion and flower organ defects, among other things ([MGBSY92, WAS+92]). Later, WUSCHEL (WUS) and its counterpart, CLAVATA3 (CLV3) are up regulated in the central zone and the stem cell layers of the flower meristem, respectively. Both genes have distinctive, central expression patterns and interact in a negative feedback loop which specifies and maintains a pool of stem cells in the meristem. Mutations in WUS produce a premature differentiation of the stem cells, while clv3 mutants expand the stem cell zone ([MSH+98, SLH+00, YTR10]). Finally, the flower meristem will differentiate into 4 annular, concentric zones known as whorls, where the flower organs (sepals, petals, stamens and carpels) will develop. The control of these whorls is regulated by three families of genes, called A, B and C, as described in the so-called ABC model ([**?**]). The A genes, AP1 and APETALA (AP2) define the sepals. A plus B genes (i.e., APETALA3 (AP3) and PISTILLATA (PI)) characterize the petals. The C gene, AGAMUS (AG), together with B genes define the stamens while C alone defines the carpels (Fig.1.4 ([CM91, BSM91]). Hence, the presence of different sets of genes, differentially characterizes the flower meristem spatially and temporally.

So, how do genes dynamically obtain their spatial and temporal expression patterns? Experimental research has demonstrated that genes interact with each other at many different levels, including chromatin modifications, physical interaction and transcriptional and posttranscriptional regulation. All these interactions are indispensable to regulate their spatio-temporal expression patterns.

1.3.2 Modules controlling development

Interestingly, at the beginning of flower development, auxin promotes directly LFY expression thought its signaling pathway ([YWW+13]). However, it has been clearly

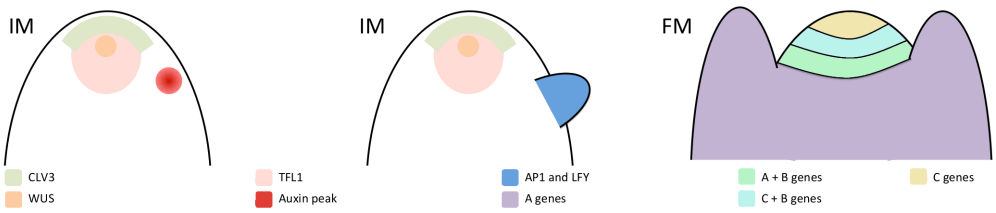

Figure 1.4: Gene expression patterns during flower transition and development. IM = Inflorescence meristem and FM = Flower meristem.

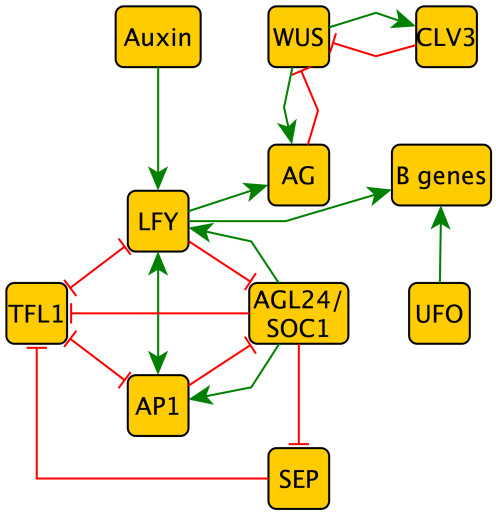

Figure 1.5: Graph of the GRN that regulates flower transition and development. Nodes represent the genes and the edges the interactions among them. Red and green edges stand for negative and positive interactions, respectively.

demonstrated, that LFY expression, not only depends on auxin concentration. LFY and AP1 are inhibited by and inhibit TFL1, a negative regulator of flowering time. On the other hand, AP1 and LFY positively up regulate each other ([RAV+98, RBC99, LGBP+99, KWMno+10, WABBe+11]). In agreement with this, TFL1 expression is complementary with AP1 and LFY expression. The expression domains of the latter two genes greatly overlap within the flower meristem, while TFL1 is exclusively expressed in the inflorescence meristem [RBC99]. Moreover, AGL24 and SOC1, two flower inducing genes, positively regulate AP1 and LFY ([GGK12, LCE+08]), and together with AP1, they act to repress TFL1 ([LTB+13]). Interestingly, while SOC1 and AGL24 regulate each other positively ([LCE+08]), creating another positive feedback loop, AP1 represses them ([LZBD+07]). Consequently, AGL24 and SOC1 are down regulated once AP1 expression is established. AGL24 and SOC1 down-regulation is important for flower development to proceed, given that AGL24 and SOC1 inhibits the SEPALLATA (SEP) genes, which are important for ABC genes up regulation ([PDB+00, DPR+04]). Once AGL24 and SOC1 are down-regulated, SEP genes repress TFL1 ([LTB+]).

As flower development continues, still in early flower developmental phases, WUS and CLV3 expression is up regulated in the flower meristem. WUS and CLV3 form

a loop, where WUS, non-cell autonomously, up regulates CLV3 while CLV3 inhibits WUS expression. These regulations create a negative feedback loop, which controls the size of the stem cell niche and the number of stem cells within it ([MSH+98, SLH+00, IMOT09]). In the flower meristem, WUS expression is not only important for stem cell maintenance, but also to induce AG in conjunction with LFY ([LHH+01]). During flower organ development, AG and AP1 delimit two main regions, since they repress each other. The B genes expression, which shares a part of its expression domain with the A genes and another with the C genes, also depends on the expression of a different set of genes, like UFO ([CTHI08]). Close to the end of flower patterning, AG turns off WUS. This is an important step to complete and end flower development (Fig.1.5)([LBJurL01]).

Finally, it is important to note that genes and hormones also communicate. LFY modifies the metabolism, transport and signaling of auxin ([LZL+13, WABBe+11]). AP1 modifies gibberellins metabolism and response ([KWMno+10]). Gibberellins also act as a flowering inductor by promoting genes like SOC1 ([MSL+03]) and LFY expression ([BGN+98]). And the CLV3/WUS regulatory module interacts with the cytokinin's metabolism and signaling pathway ([CGT+12]), indicating that gene and hormonal regulation are not independent processes.

Due to the high gene interconnectivity, the non-linearity of the gene interactions and the complexity of the molecular regulation, computational and mathematical models are necessary to deeply study them in a more integrated way. Many different approaches can be taken while modelling molecular regulation. Here we will focus on two of the most used ones, Boolean and ordinary differential equations (ODEs) gene regulatory network (GRN) models (for a more comprehensive review about GRN modelling formalism see e.g. ([DJ02]), see Math-Box *Mathematical modelling of regulatory networks*). Both, Boolean and ODEs models provide meaningful information about the system dynamics. Consequently, they have been already employed for a wide variety of systems, including flower development. For example, a flowering transition GRN has been modeled recently ([JPL+13]) while the flower organ development GRN has been modeled for a long time with different approaches ([MAB98, ESPLAB04, vMvDdG+10]).

Mathematical modelling of regulatory networks

Mathematically, a network of n genes interacting with each other is represented by a list (or *vector*) of n numbers

$$X = (X_1, \ldots, X_n)\,,$$

where each X_i represents the level of expression, or activity, or the gene i.
The entries X_i are sometimes continuous, typically interpreted as the concentration of the mRNA, or protein coded by gene i. This leads to a continuous state space (see Math-Box 'Dynamical Systems' above) of the form $\mathbb{R}^n$.
The entries X_i can also be discrete, representing the gene i being transcribed "Not at all (0), A little (1), A little more (2)..." with a finite number of levels. The most common case, called Boolean, is when X_i takes only to values 0 (not transcribed) or 1 (transcribed), with a state space $\{0, 1\}^n$.
In both cases, referred to as 'continuous' and 'discrete' hereafter, the evolution of the network is defined as a dynamical system (see frames 'Dynamical Systems').

... *continued :* Mathematical modelling of regulatory networks

In the discrete case, one thus needs a successor map

$$F : \{0,1\}^n \to \{0,1\}^n.$$

In the context of gene network modelling, one refers to the flow induced by this map as **synchronous**, because this updates all the genes simultaneously at each time step. An alternative approach, where it is deemed more realistic to update at most one gene at a given time, is called **asynchronous**: only one coordinate F_i of the map F is applied at each time step, all other variables being left unchanged. A rule has to be introduced to determine which variables are updated (it can be deterministic or stochastic). It is easy to prove that steady states are identical for synchronous and asynchronous updates, and are the fixed points of the successor map F.
In the continuous case, the differential equation describing the system's dynamics is usually derived from the laws of chemical kinetics. For simplicity, these laws are often simplified using 'quasi-steady state assumptions', whereby some variables are supposed to evolve so fast that they reach steady state instantly. A standard form obtained from this assumptions is the so-called Hill function:

$$h(X_i) = \frac{X_i^p}{X_i^p + \theta_i^p},$$

which rapidly increases near $X_i \approx \theta_i$ from a plateau $h \approx 0$ (when $X_i < \theta_i$) to a plateau $h \approx 1$ (when $X_i < \theta_i$). Intuitively, one can see here a connection with Boolean models. This connection can be made more precise, although this is not discussed in details in this chapter. The whole system is then described by the system of ODE

$$\frac{dX}{dt} = F(X) = (F_1(X), \ldots, F_n(X)),$$

where the jth coordinate F_j is a sum of products of terms of the form $h(X_i)$.

1.3.3 Modelling the genetic regulation of the bud fate

As stated by[Kau69] in the Boolean context, the steady states of a GRN correspond to the different gene configuration states observed in a biological system. For example, in the case of the flower meristem, they could correspond to the whorls gene configuration observed experimentally. This hypothesis has been independently corroborated by different groups (e.g., [AO03, ESPLAB04, JPL+13]).

GRN formalisms

We can build a network using the experimental information about genes interactions and gene expression patterns presented before. Let us take as an example, the expression patterns and gene interactions of AP1, LFY and TFL1, which are at the core of the transition from inflorescence meristem to floral meristem. According to the above

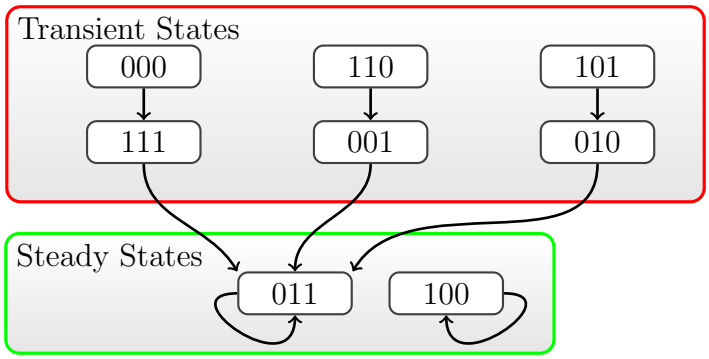

Figure 1.6: Gene transitions and steady states for the Boolean GRN example. Each node represents one state of variables TFL1, AP1 and LFY (in this order), and arrows represent the action of the successor map. The two steady states 011 and 100 are respectively interpreted as 'flower meristem' and 'inflorescence meristem'.

description, TFL1 is a negative regulator of AP1 and LFY. LFY and AP1 are negative regulators of TFL1 and positive regulators of each other (Fig.1.5). This situation can be formalized in either discrete or continuous time (see Math-Boxes *Dynamical systems: Discrete Time* and *Dynamical systems: Continuous Time*).

In discrete time, Boolean networks are often used as they are the simplest discrete modelling formalism to study GRN. The successor map is usually defined gene by gene using logical statements on how these genes are regulated. A possible set of Boolean functions describing the AP1, LFY, TFL1 network is the following:

$$\begin{aligned} TFL1(t+1) &= !AP1(t)\&!LFY(t) \\ AP1(t+1) &= !TFL1(t)\,|\,LFY(t) \\ LFY(t+1) &= !TFL1(t)\,|\,AP1(t) \end{aligned}$$

where !, & and | stand for the logical NOT, AND and OR, respectively. The state space of this system made-up of 3 boolean variables has altogether eight elements ($2^3 = 8$). For each state, one can calculate a successor using the rules above, the resulting successor map is represented graphically in Figure 1.6. In general, an analogue of this figure can be produced and recapitulates the complete dynamics of a Boolean GRN model, but in practice the state space can be too large to perform the full calculation, or represent it in a readable way. It is usually possible, though, to find the system's steady states. In our example, there are two steady states 011 and 100, which correspond to the 'inflorescence meristem' and 'flower meristem' identities (Fig.1.6).

One sees in Figure 1.6 that the Boolean representation does not allow for gradual changes of the variables. In particular, for the chosen rules the 'inflorescence meristem' state 100 has no predecessor (a situation sometimes referred to as 'garden of Eden'), so that any perturbation of this state will immediately enter the 'basin of attraction' of the other steady state. In fact, during plant development, we will transit from an 'inflorescence meristem' to a 'flower meristem' identity. However, this transition happens only when a new meristem is produced under specific conditions (i.e. high FT concentration and an auxin peak; see above and chapter 3) and not under any

type of perturbation. While there are many different way to overcome this and other limitations of the Boolean modeling approach, one of the best solutions, which gives a more gradual representation of genes dynamics, capable to overcome many of the Boolean limitations, is possible through the use of a ODEs model. In this case, the variables are the concentrations [TFL1], [AP1] and [LFY]. Using Hill functions, a set of equations analogue to the Boolean model above can be written in the following form:

$$\begin{aligned}
\frac{d[TFL1]}{dt} &= \frac{\theta_{AP1}^p}{[AP1]^p + \theta_{AP1}^p} \frac{\theta_{LFY}^p}{[LFY]^p + \theta_{LFY}^p} - \delta_{TFL1}[TFL1], \\
\frac{d[AP1]}{dt} &= \frac{1}{2}\left(\frac{[LFY]^p}{[LFY]^p + \theta_{LFY}^p} + \frac{\theta_{TFL1}^p}{[TFL1]^p + \theta_{TFL1}^p}\right) - \delta_{AP1}[AP1], \\
\frac{d[LFY]}{dt} &= \frac{1}{2}\left(\frac{[AP1]^p}{[AP1]^p + \theta_{AP1}^p} + \frac{\theta_{TFL1}^p}{[TFL1]^p + \theta_{TFL1}^p}\right) - \delta_{LFY}[LFY],
\end{aligned}$$

where δ_X accounts for the degradation of each of the genes in the network. The value of the parameters need to be obtained from experiments or estimated. There are different parameter estimation methods (e.g. [SGH12]). For this example, θ_X values, which represent the substrate concentration at which the reaction rate is half its maximal, was set to 1, all decays $\delta_X = 0.3$ and the Hill coefficient $p = 3$. Solving the system above cannot be achieved by hand any more, but numerical simulations give steady states which are analogue to the Boolean case Fig.1.8. Importantly, with the ODEs model, we can observe the expected transitions, from an inflorescence to a flower meristem identity. However, in the continuous case, the transition can be simulated in a more realistic way. For example, the transition can be achieved by gradually modifying the initial TFL1 concentration, as observed in Fig.1.8. At a particular threshold, a transition is made from a steady state with low TFL1 concentration to a steady state with high TFL1 concentration. Hence, we can see here that the use of an ODE model makes it possible to solve two problems: 1) identify perturbations that are able to modify the steady state of the system and 2) provide plausible mechanisms that reproduce developmental transitions in a realistic way.

Regulatory networks have usually complex structures and behaviors and cannot readily be analyzed in a simple qualitative manner. Instead, it is most of the time necessary to quantify GRNs in order to analyze and understand their properties. It is not obvious for example that a network such as the one presented in Figure 1.5, built from different sources of information, would eventually be self-consistent. The use of models allows us to study such consistencies and analyze emerging properties of the GNR. In the next section we will how such analyses can be performed with the aid of a network modeling approach.

Analysis of network properties

As observed from the previous examples, even if we are dealing with a simple network motif, some interesting properties, like the steady states, can be studied in a systematic way. Likewise, from the models other network properties can be analyzed in order to validate, predict or understand the molecular mechanisms. For example, a posterior

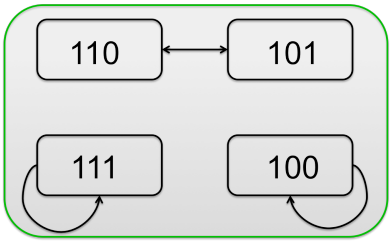

Figure 1.7: Steady states obtained for an over-expression of TFL1.

analysis that we could perform in any biological GRN is a mutant analysis. In both, continuous and discrete networks, fixing the nodes values to 0 simulates loss-of-function mutants. While the over expression of a gene is simulated by fixing its value to 1 in the Boolean case, and to a high value in the continuous case. For example, we could simulate TFL1 over expression. According to experimental research, TFL1's over expression delays LFY and AP1 up regulation, but does not forbid it ([RAV+98]), suggesting that the positive feedback loop between LFY and AP1 is stronger that TFL1 repression. When we perform this simulation using the Boolean or the ODEs model, TFL1 over expression does not forbid the AP1 and LFY upregulation. However, in the Boolean case we obtain a biologically meaningless cyclic steady state (1.7), which appears due to their time limitation and synchronous gene updating. In contrast, with the ODEs modelling approximation we do not obtain any unrealistic cyclic steady state. In fact, many mutant effects are easier to represent in a continuous framework, and can be used to determine plausible ranges for the parameters. The list of properties that we can analyze using GRN model is large, and includes structural (e.g., connectivity, clustering, network motifs) and dynamical (evolvavility, robustness, stability) properties.

In both the continuous and the discrete case, in the TFL1 over expression simulation, we find that the steady states with TFL1 and the other with all three genes up regulated are congruent with the experimental information. Both, steady states and mutant simulations are important to validate the model. Incongruences between the network results and the experimental data suggest that the model is incorrect and needs to be modified.

The use of modeling approaches to understand the molecular mechanisms behind the developmental processes is necessary. As observed from our examples, even with a simple network motif, there are some non-trivial behaviours, like the appearance of different steady states and the effect of the mutants. We only used a toy model, however, many research groups have tried to have a more comprehensive understanding of the flowering transition and other developmental processes ([MAB98, AO03, ESPLAB04, vMvDdG+10, CGT+12, JPL+13]). The knowledge generated from this work has provided insightful and deeper information.

Importantly, with both Boolean and continuous modeling approaches, we can sometimes obtain equivalent information. However, discrete formalisms, including the Boolean one, are by nature qualitative and there is time is not represented explicitly. Moreover, in general the update of the network state is synchronous for all the nodes. These limitations can generate artefacts in the network dynamics, like the unrealistic transitory states described above. We observed for example that, if we start from the state AP1 = 1, LFY = 0 and TFL1 = 1 in the Boolean version of the model, we will pass a transitory state with AP1 = 0, LFY = 1 and TFL1 = 0 before reaching the steady state

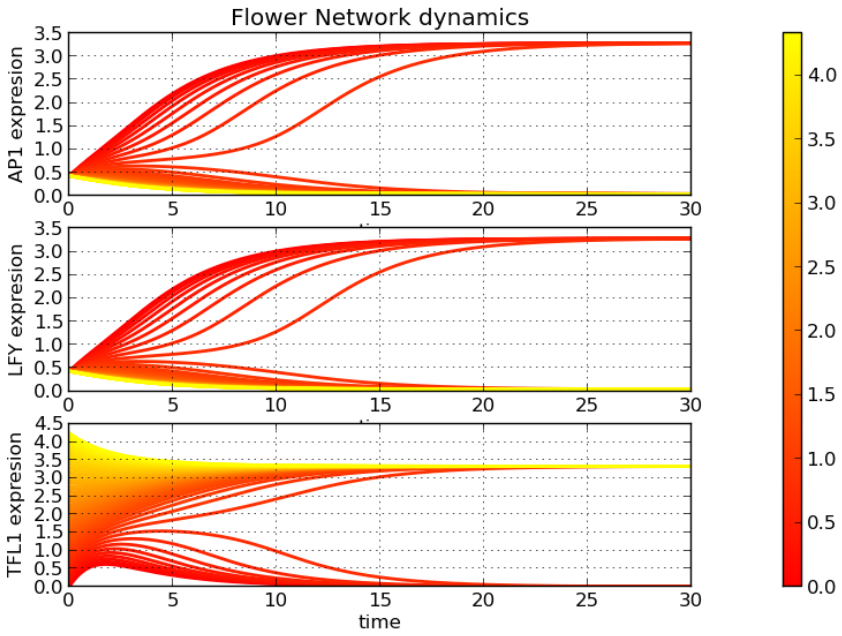

Figure 1.8: Time course for each of the three genes, using the ODE model. Parameters as given in the text. The colorbar indicate changes in the initial concentration of TFL1, which is gradually increased from 0 to 4. Low values of TFL1 lead to a steady state analogue to the Boolean 011, while high values lead to the analogue of 100.

configuration (Fig.1.6). The AP1 down regulation in the transitory state has never been observed experimentally during flower transition, and in fact, it is not observed in the continuous version of the model (Fig.1.8), indicating that it is an artefact of the Boolean formalism.

Thus, even when there are a number of possibilities to overcome discrete modeling limitations, like translating the Boolean model into a qualitative continues one and using an asynchronous update of the gene's values, ODEs models directly override many of the discrete formalism limitations at the cost of many parameters which are usually unavailable and need to be estimated. This is the reason why the modeling formalism must be selected depending on the available data and the research aim. Networks can be used to study gene dynamics, development robustness, molecular pathways architecture, to predict missing, wrong or incoherente information, among many other things. They provide an extremely useful tool for the study of any molecular process.

Dynamical Systems: Discrete Time

The archetype of discrete time is given by integer numbers, i.e. $T = \mathbb{N}$ or $\mathbb{Z}$. In that case, one can use the flow to define a notion of **successor** map, denoted $F : S \to S$. Given a state s, this map returns the new state of the system after 1 unit of time:

$$F(x) = \Phi(x, 1).$$

Very often, discrete time dynamical systems will be presented directly in terms of their successor map instead of the flow Φ. If needed, the flow can always be retrieved by repeatedly applying the successor map: $\Phi(x, t) = \underbrace{F \circ F \circ \cdots F}_{t \text{ times}}(x)$.

Example (Lindenmayer Algae): This system represents the shape of an algae using a word written with two symbols 'A' and 'B'. The state space is thus the set of all words that can be written with these two symbols, denoted $\{A, B\}^*$. The successor map is defined in two steps. First, one introduces the two rules:

A $\longrightarrow$ AB
B $\longrightarrow$ A

The successor map is the transformation which, given a word $w \in \{A, B\}^*$ returns the new word obtained by replacing every occurrence of 'A' by 'AB', and then every occurrence of 'B' by 'A'.
This system is usually considered only with the initial state 'A' and not the whole state space (i.e. one considers a single trajectory and in this case the notion of stability is not relevant), and defining the flow would introduce unnecessary complications. ◇

The previous example has a discrete state space. One can also have a discrete time and a continuous state space.

Example (logistic map): The logistic map $F(x) = \lambda x(1 - x)$ is a famous dynamical system, representing the evolution of a population (of size x) in a medium with limited resources (represented by the term $(1 - x)$).

This system has two steady states 0 and $x_\lambda = \frac{\lambda - 1}{\lambda}$, which are the solutions of the fixed point equation $F(x) = x$. One can prove that 0 is stable for $0 < \lambda \leq 1$ and unstable otherwise. Also, x_λ is stable for $1 < \lambda \leq 3$ and unstable for $\lambda > 3$. In the latter case, the trajectories of this system can become very complicated, despite its simple formulation. ◇

The example above illustrates an important concept: a **bifurcation** occurs when the number or stability of steady states in a system change for a particular value of some parameter. A parameter is a number that appears in the formulas defining a dynamical system and which does not evolve in time (i.e. it is not a variable).

Dynamical Systems: Continuous Time

The archetype of continuous time is the set of real numbers, i.e. $T = \mathbb{R}$. In this case, one cannot define a successor, because for any positive time t one can find a shorter time t' that would be a nearer successor, and the limit $t \to 0$ gives the current time, hence not a successor. However, one knows from calculus that the following limit makes sense, as the derivative

$$\frac{\partial \Phi(x,t)}{\partial t} = \lim_{dt \to 0} \frac{\Phi(x, t+dt) - \Phi(x,t)}{dt}.$$

Continuous time dynamical systems are very often presented in terms of this derivative, the rate of change of the state. A function F is used as an evolution rule, providing the rate of change for each state x of the system. This provides us with a **differential equation** of the form

$$\frac{\partial x}{\partial t} = F(x).$$

Then, the notion of flow is identical to the concept of solution of the differential equation above. Some standard terminology is associated with differential equations: the state x is usually a vector $x = (x_1, x_2, \ldots, x_n)$ of real numbers which depends on time and space, i.e. it is a function $x(X, Y, Z, t)$ where X, Y, Z are spatial coordinates. If the right-hand side $F(x)$ involves partial derivatives other than $\partial/\partial t$ (e.g. $\partial/\partial X$, $\partial^2/\partial X^2$,...) the model is a system of **partial differential equations**, abbreviated PDE. Otherwise, one uses the the term **ordinary differential equations**, abbreviated ODE, and the notation is slightly altered:

$$\frac{dx}{dt} = F(x).$$

Example (Reaction-Diffusion): The diffusion in space of a substance of concentration $c(X, Y, Z, t)$ is modelled by the Laplacian operator (in Cartesian coordinates)

$$\triangle c = \frac{\partial^2 c}{\partial X^2} + \frac{\partial^2 c}{\partial Y^2} + \frac{\partial^2 c}{\partial Z^2}.$$

Alternatively, one may consider a discretized spatial domain, with a finite number of sites $i \in \{1, ..., N\}$ (for instance cells in a tissue) with concentration c_i in site i. In this framework each site i has a set $\mathcal{N}_i$ of neighbours and diffusion is modelled by

$$\triangle c = \sum_{j \in \mathcal{N}_i} (c_j - c_i)$$

The notation $\triangle$ is ambiguous above but would always be clear in a given context. When two substances of concentration c_A and c_B interact chemically and diffuse in space, their evolution is described by a system of the form:

$$\begin{cases} \dfrac{\partial c_A}{\partial t} &= F(c_A, c_B) + D_A \bigtriangledown c_A \\ \dfrac{\partial c_B}{\partial t} &= G(c_A, c_B) + D_B \triangle c_B \end{cases}$$

... *continued :* Dynamical Systems: Continuous Time

where D_A and D_B are the diffusion rates of the two substances and F, G functions represent the kinetics of their interactions. This class of model, first proposed by Alan Turing, is capable of generating a large variety of spatial patterns, modelled as steady states of the two equations above. The ratio between the two diffusion rates is often used as a parameter to study bifurcations, which in this context are interpreted as changes in the spatial patterns of substances A and B.
Note that with a discrete spatial domain, the system above is in fact a system of ODE and the notation d/dt should be used. ◇

Remark: With differential equations, steady states can be found by solving a system of algebraic equations. Indeed, by definition a steady state is such that its rate of change is zero, i.e. a solution of $F(x) = 0$. These solutions can sometimes be computed by hand.

1.4 Conclusion

In this chapter we have discussed how two key processes in flower primordium formation can be described and modeled in a quantitative way. In the first section, we briefly reviewed models that make it possible to explain the dynamic accumulation of auxin at the SAM. We described the main assumptions about auxin transport that have been proposed and tested in the literature (concentration-based and flux-based hypotheses). Models make it possible to check whether these assumptions expressed in terms of local cell-to-cell interaction rules lead to consistent patterning in the growing tissue as emerging properties. When compared to data, each model has its own strengths and weaknesses. However, in the current state of our knowledge, it is difficult to identify clearly whether the assumptions underlying a particular transport model are more realistic than that of others. To proceed further, two main avenues must be explored: i) we first need to get deeper knowledge on the biological processes underlying the transport between cells. ii) We also need to get better mathematical insight into these complex models mixing spatial structure, growth, biochemical reactions and feedback loops between these elements.

Based on the assumption that a flower is initiated at the SAM downstream of auxin spatial accumulation, we then investigated the gene regulatory network that controls the initial steps of flower development and differentiation. In a simplified form, this network contains a dozen of actors interacting with each other in space and time. The understanding of such a complex system here also requires a modeling approach in order to quantify these interactions and analyze their properties. We briefly presented the two main formalisms that are used to model GRN: the Boolean and the ODE formalisms. We illustrated on a sub-module of the flower GRN both types of models and discussed their main advantages and drawbacks. We showed how manipulations of the network models can be used to make predictions corresponding to possible biological manipulations of the GRN (e.g. loss-of-function mutants).

An integrated view of flower initiation would require to address other important biological processes. For example, a mechanical model would be required to study how the flower dome is bulging out from the meristem dome (and recursively how the young organs such as sepals, petals, are physically emerging from the flower primordium). Such models are currently being developed (e.g [HHJ$^+$08, BKJ14, BCA$^+$15] and provide a rigorous basis to quantify further the effect of forces on the shaping of organs. These models will also need to be coupled, for example by connecting auxin transport models to gene regulatory networks on realistic 3-dimensional structures obtained from confocal microscopy (e.g. [FDM$^+$10, BdRRKK$^+$15]). This will make it possible to test the consistency between several modeling modules in the context of a more integrated spatio-temporal understanding of flower development. Of course to do so, simplifications will have to be operated on the detailed models, adaptation between their typical time and spatial scales will have to be considered. As a result, it will be possible to compare and assess the output of model simulations with observations of development in a precise quantitative manner, leading to the possibility to develop further the models as companion and powerful tools for the study of development.

Bibliography

[ABBitCPe+10] E R Alvarez-Buylla, M Ben i tez, A Corvera-Poir e, A Chaos Cador, S de Folter, A Gamboa de Buen, A Garay-Arroyo, B Garc i a Ponce, F Jaimes-Miranda, R V P e rez Ruiz, A Piñeyro-Nelson, and Y E S a nchez Corrales. Flower development, 2010.

[ABdRS+13] K Abley, Pierre Barbier de Reuille, D Strutt, A Bangham, Przemyslaw Prusinkiewicz, A F M Maree, V A Grieneisen, and E Coen. An intracellular partitioning-based framework for tissue cell polarity in plants and animals. *Development*, 140(10):2061–2074, April 2013.

[AO03] R Albert and H G Othmer. The topology of the regulatory interactions predicts the expression pattern of the segment polarity genes in Drosophila melanogaster. *Journal of Theoretical Biology*, 223(1):1–18, July 2003.

[BCA+15] Frédéric Boudon, Jérôme Chopard, Olivier Ali, Benjamin Gilles, Olivier Hamant, Arezki Boudaoud, Jan Traas, and Christophe Godin. A Computational Framework for 3D Mechanical Modeling of Plant Morphogenesis with Cellular Resolution. *PLoS computational biology*, 11(1):e1003950–16, January 2015.

[BdRBCL+06] Pierre Barbier de Reuille, Isabelle Bohn-Courseau, Karin Ljung, Halima Morin, Nicola Carraro, Christophe Godin, and Jan Traas. Computer simulations reveal properties of the cell-cell signaling network at the shoot apex in Arabidopsis. *Proceedings of the National Academy of Sciences*, 103(5):1627–1632, January 2006.

[BdRRKK+15] Pierre Barbier de Reuille, Anne-Lise Routier-Kierzkowska, Daniel Kierzkowski, George W Bassel, Thierry Schüpbach, Gerardo Tauriello, Namrata Bajpai, Sören Strauss, Alain Weber, Annamaria Kiss, Agata Burian, Hugo Hofhuis, Aleksandra Sapala, Marcin Lipowczan, Maria B Heimlicher, Sarah Robinson, Emmanuelle M Bayer, Konrad Basler, Petros Koumoutsakos, Adrienne Hk Roeder, Tinri Aegerter-Wilmsen, Naomi Nakayama, Miltos Tsiantis, Angela Hay, Dorota Kwiatkowska, Ioannis Xenarios, Cris Kuhlemeier, and Richard S Smith. MorphoGraphX: A platform for quantifying morphogenesis in 4D. *eLife*, 4, 2015.

[BGB+08] Katherine Bainbridge, Soazig Guyomarc'h, Emmanuelle Bayer, Ranjan Swarup, Malcolm Bennett, Therese Mandel, and Cris Kuhlemeier.

Auxin influx carriers stabilize phyllotactic patterning. *Genes & development*, 22(6):810–823, March 2008.

[BGN+98] M A Blázquez, R Green, O Nilsson, M R Sussman, and D Weigel. Gibberellins promote flowering of arabidopsis by activating the LEAFY promoter. *The Plant cell*, 10(5):791–800, May 1998.

[BKJ14] Behruz Bozorg, Pawel Krupinski, and Henrik Jönsson. Stress and strain provide positional and directional cues in development. *PLoS computational biology*, 10(1):e1003410, January 2014.

[BP13] Siobhan A Braybrook and Alexis Peaucelle. Mechano-Chemical Aspects of Organ Formation in Arabidopsis thaliana: The Relationship between Auxin and Pectin. *PloS one*, 8(3):e57813, March 2013.

[BRB+11] Gemma D Bilsborough, Adam Runions, Michalis Barkoulas, Huw W Jenkins, Alice Hasson, Carla Galinha, Patrick Laufs, Angela Hay, Przemyslaw Prusinkiewicz, Miltos Tsiantis, and R A. Model for the regulation of Arabidopsis thaliana leaf margin development. *Proceedings of the National Academy of Sciences*, 108(8):3424–3429, February 2011.

[BSM91] J L Bowman, D R Smyth, and E M Meyerowitz. Genetic interactions among floral homeotic genes of Arabidopsis. *Development*, 112(1):1–20, May 1991.

[BSM+09] E M Bayer, R S Smith, T Mandel, N Nakayama, M Sauer, Przemyslaw Prusinkiewicz, and C Kuhlemeier. Integration of transport-based models for phyllotaxis and midvein formation. *Genes & development*, 23(3):373–384, January 2009.

[CGT+12] Vijay S Chickarmane, Sean P Gordon, Paul T Tarr, Marcus G Heisler, and Elliot M Meyerowitz. Cytokinin signaling as a positional cue for patterning the apical-basal axis of the growing Arabidopsis shoot meristem. *Proceedings of the National Academy of Sciences of the United States of America*, February 2012.

[Cha12] J W Chandler. Floral meristem initiation and emergence in plants. *Cellular and Molecular Life Sciences*, 69(22):3807–3818, November 2012.

[CM91] E Coen and E Meyerowitz. The war of the whorls: genetic interactions controlling flower development. *Nature*, 353()(6339):31–37–, September 1991.

[CTHI08] E Chae, Q K Tan, T A Hill, and V F Irish. An Arabidopsis F-box protein acts as a transcriptional co-factor to regulate floral development. *Development*, 135(7):1235–1245, April 2008.

[DJ02] Hidde De Jong. Modeling and simulation of genetic regulatory systems: a literature review. *Journal of computational biology : a journal of computational molecular cell biology*, 9(1):67–103, 2002.

[DPR+04] G S Ditta, A Pinyopich, P Robles, S Pelaz, and M F Yanofsky. The SEP4 gene of Arabidopsis thaliana functions in floral organ and meristem identity. *Current biology*, 14(21):1935–1940, November 2004.

[ESPLAB04] Carlos Espinosa-Soto, Pablo Padilla-Longoria, and Elena R Alvarez-Buylla. A gene regulatory network model for cell-fate determination during Arabidopsis thaliana flower development that is robust and recovers experimental gene expression profiles. *THE PLANT CELL ONLINE*, 16(11):2923–2939, November 2004.

[FDM+10] Romain Fernandez, Pradeep Das, Vincent Mirabet, Eric Moscardi, Jan Traas, Jean-Luc Verdeil, Grégoire Malandain, and Christophe Godin. Imaging plant growth in 4D: robust tissue reconstruction and lineaging at cell resolution. *Nature methods*, 7(7):547–553, June 2010.

[Feu06] F Feugier. Models of Vascular Pattern Formation in Leaves. *PhD Thesis*, 2006.

[FFM15] Chrystel Feller, Etienne Farcot, and Christian Mazza. Self-Organization of Plant Vascular Systems: Claims and Counter-Claims about the Flux-Based Auxin Transport Model. *PloS one*, 10(3):e0118238–18, March 2015.

[FI06] François G Feugier and Yoh Iwasa. How canalization can make loops: A new model of reticulated leaf vascular pattern formation. *Journal of Theoretical Biology*, 243(2):235–244, November 2006.

[FMI05] François G Feugier, A Mochizuki, and Y Iwasa. Self-organization of the vascular system in plant leaves: Inter-dependent dynamics of auxin flux and carrier proteins. *Journal of Theoretical Biology*, 236(4):366–375, October 2005.

[FY13] E Farcot and Y Yuan. Homogeneous auxin steady states and spontaneous oscillations in flux-based auxin transport models. *SIAM Journal on Applied Dynamical Systems*, 2013.

[GGK12] V Grandi, V Gregis, and M M Kater. Uncovering genetic and molecular interactions among floral meristem identity genes in Arabidopsis thaliana. *Plant Journal*, 69(5):881–893, March 2012.

[HHJ+08] O Hamant, M G Heisler, Henrik Jönsson, P Krupinski, M Uyttewaal, P Bokov, F Corson, P Sahlin, A Boudaoud, E M Meyerowitz, Y Couder, and J Traas. Developmental Patterning by Mechanical Signals in Arabidopsis. *Science (New York, NY)*, 322(5908):1650–1655, December 2008.

[HHK+10] Marcus G Heisler, Olivier Hamant, Pawel Krupinski, Magalie Uyttewaal, Carolyn Ohno, Henrik Jönsson, Jan Traas, and Elliot M Meyerowitz. Alignment between PIN1 polarity and microtubule orientation in the shoot apical meristem reveals a tight coupling between morphogenesis and auxin transport. *PLoS Biol*, 8(10):e1000516, 2010.

[IMOT09] M Ikeda, N Mitsuda, and M Ohme-Takagi. Arabidopsis WUSCHEL is a bifunctional transcription factor that acts as a repressor in stem cell regulation and as an activator in floral patterning. *The Plant cell*, 21(11):3493–3505, November 2009.

[JHS+06] Henrik Jönsson, Marcus G Heisler, Bruce E Shapiro, Elliot M Meyerowitz, and Eric Mjolsness. An auxin-driven polarized transport model for phyllotaxis. *Proceedings of the National Academy of Sciences*, 103(5):1633–1638, January 2006.

[JPL+13] K E Jaeger, N Pullen, S Lamzin, R J Morris, and P A Wigge. Interlocking feedback loops govern the dynamic behavior of the floral transition in Arabidopsis. *The Plant cell*, 25(3):820–833, March 2013.

[Kau69] S Kauffman. Homeostasis and differentiation in random genetic control networks. *Nature*, 224(5215):177–178, October 1969.

[KB06] Eric M Kramer and Malcolm J Bennett. Auxin transport: a field in flux. *Trends in Plant Science*, 11(8):382–386, August 2006.

[KJ10] P Krupinski and Henrik Jönsson. Modeling Auxin-regulated Development. *Cold Spring Harbor Perspectives in*, January 2010.

[Kra04] Eric M Kramer. PIN and AUX/LAX proteins: their role in auxin accumulation. *Trends in Plant Science*, 9(12):578–582, December 2004.

[KWMno+10] K Kaufmann, F Wellmer, J M Mui n o, T Ferrier, S E Wuest, V Kumar, A Serrano-Mislata, F Madue n o, P Krajewski, E M Meyerowitz, G C Angenent, and J L Riechmann. Orchestration of floral initiation by APETALA1. *Science*, 328(5974):85–89, April 2010.

[LBJurL01] M Lenhard, A Bohnert, G J u rgens, and T Laux. Termination of stem cell maintenance in Arabidopsis floral meristems by interactions between WUSCHEL and AGAMOUS. *Cell*, 105(6):805–814, June 2001.

[LCE+08] C Liu, H Chen, H L Er, H M Soo, P P Kumar, J H Han, Y C Liou, and H Yu. Direct interaction of AGL24 and SOC1 integrates flowering signals in Arabidopsis. *Development*, 135(8):1481–1491, April 2008.

[LGBP+99] S J Liljegren, C Gustafson-Brown, A Pinyopich, G S Ditta, and M F Yanofsky. Interactions among APETALA1, LEAFY, and TERMINAL FLOWER1 specify meristem fate. *The Plant cell*, 11(6):1007–1018, June 1999.

[LHH+01] J U Lohmann, R L Hong, M Hobe, M A Busch, F Parcy, R Simon, and D Weigel. A molecular link between stem cell regulation and floral patterning in Arabidopsis. *Cell*, 105(6):793–803, June 2001.

[LTB+] C Liu, Z W Teo, Y Bi, S Song, W Xi, X Yang, Z Yin, and H Yu. A conserved genetic pathway determines inflorescence architecture in Arabidopsis and rice.

[LTB+13] Chang Liu, Zhi Wei Norman Teo, Yang Bi, Shiyong Song, Wanyan Xi, Xiaobei Yang, Zhongchao Yin, and Hao Yu. A Conserved Genetic Pathway Determines Inflorescence Architecture in Arabidopsis and Rice. *Developmental Cell*, 24(6):612–622, March 2013.

[LTY09] C Liu, Z Thong, and H Yu. Coming into bloom: the specification of floral meristems. *Development*, 136(20):3379–3391, October 2009.

[LZBD+07] C Liu, J Zhou, K Bracha-Drori, S Yalovsky, T Ito, and H Yu. Specification of Arabidopsis floral meristem identity by repression of flowering time genes. *Development*, 134(10):1901–1910, May 2007.

[LZL+13] W Li, Y Zhou, X Liu, P Yu, J D Cohen, and E M Meyerowitz. LEAFY controls auxin response pathways in floral primordium formation. *Sci. Signal.*, 6(277):ra23.cr, May 2013.

[MAB98] L Mendoza and E R Alvarez-Buylla. Dynamics of the genetic regulatory network for Arabidopsis thaliana flower morphogenesis. *Journal of Theoretical Biology*, 193(2):307–319, July 1998.

[MGBSY92] M A Mandel, C Gustafson-Brown, B Savidge, and M F Yanofsky. Molecular characterization of the Arabidopsis floral homeotic gene APETALA1. *Nature*, 360(6401):273–277, November 1992.

[Mit80] G J Mitchison. A model for vein formation in higher plants. *Philosophical Transactions of the Royal Society of London B Biological Sciences*, 207:79–109, 1980.

[Mit81] G J Mitchison. The polar transport of auxin and vein pattern in plants. *Philosophical Transactions of the Royal Society of London B Biological Sciences*, 295:461–471, 1981.

[MSH+98] K F Mayer, H Schoof, A Haecker, M Lenhard, G J u rgens, and T Laux. Role of WUSCHEL in regulating stem cell fate in the Arabidopsis shoot meristem. *Cell*, 95(6):805–815, December 1998.

[MSL+03] J Moon, S S Suh, H Lee, K R Choi, C B Hong, N C Paek, S G Kim, and I Lee. The SOC1 MADS-box gene integrates vernalization and gibberellin signals for flowering in Arabidopsis. *Plant Journal*, 35(5):613–623, September 2003.

[PBLG+11] Alexis Peaucelle, Siobhan A Braybrook, Laurent Le Guillou, Emeric Bron, Cris Kuhlemeier, and Herman Höfte. Pectin-Induced Changes in Cell Wall Mechanics Underlie Organ Initiation in Arabidopsis. *Curr Biol*, 21(20):1720–1726, October 2011.

[PCS+09] Przemyslaw Prusinkiewicz, Scott Crawford, Richard S Smith, Karin Ljung, Tom Bennett, Veronica Ongaro, and Ottoline Leyser. Control of bud activation by an auxin transport switch. *Proceedings of the National Academy of Sciences of the United States of America*, 106(41):17431–17436, October 2009.

[PDB+00] S Pelaz, G S Ditta, E Baumann, E Wisman, and M F Yanofsky. B and C floral organ identity functions require SEPALLATA MADS-box genes. *Nature*, 405(6783):200–203, May 2000.

[Rav75] J Raven. Transport of indolacetic acid in plant cells in relation to pH and electrical gradients, and its significance for polar IAA transport. *New Phyotologist*, 74:163–172, 1975.

[RAV+98] O J Ratcliffe, I Amaya, C A Vincent, S Rothstein, R Carpenter, E S Coen, and D J Bradley. A common mechanism controls the life cycle and architecture of plants. *Development*, 125(9):1609–1615, May 1998.

[RBC99] O J Ratcliffe, D J Bradley, and E S Coen. Separation of shoot and floral identity in Arabidopsis. 126(6):1109–1120, March 1999.

[RFL+05] Adam Runions, Martin Fuhrer, Brendan Lane, Pavol Federl, Anne-Gaëlle Rolland-Lagan, Przemyslaw Prusinkiewicz, Martin Fuhrer, and Anne-Gaëlle Rolland-Lagan. Modeling and visualization of leaf venation patterns. *ACM Transactions on Graphics (TOG)*, 24(3):702–711, July 2005.

[RLP05] A G Rolland-Lagan and Przemyslaw Prusinkiewicz. Reviewing models of auxin canalization in the context of leaf vein pattern formation in Arabidopsis. *The Plant journal : for cell and molecular biology*, 44(5):854–865, December 2005.

[RMK00] Didier Reinhardt, Therese Mandel, and Cris Kuhlemeier. Auxin Regulates the Initiation and Radial Position of Plant Lateral Organs. *The Plant cell*, 12(4):507–518, April 2000.

[RPS+03] Didier Reinhardt, Eva-Rachele R Pesce, Pia Stieger, Therese Mandel, Kurt Baltensperger, Malcolm Bennett, Jan Traas, Ji i Friml, and Cris Kuhlemeier. Regulation of phyllotaxis by polar auxin transport. *Nature*, 426(6964):255–260, November 2003.

[RS74] P Rubery and A Sheldrake. Carrier-mediated auxin transport. *Planta*, 118(2):101–121, 1974.

[RSP14] Adam Runions, Richard S Smith, and Przemyslaw Prusinkiewicz. Computational Modelsof Auxin-Driven Development. In *Auxin and Its Role in Plant Development*, pages 315–357. May 2014.

[SAB+14] Massimiliano Sassi, Olivier Ali, Frédéric Boudon, Gladys Cloarec, Ursula Abad, Coralie Cellier, Xu Chen, Benjamin Gilles, Pascale Milani, Jiri Friml, Teva Vernoux, Christophe Godin, Olivier Hamant, and Jan Traas. An Auxin-Mediated Shift toward Growth Isotropy Promotes Organ Formation at the Shoot Meristem in Arabidopsis. *Current biology*, 24(19):2335–2342, June 2014.

[Sac69] T Sachs. Polarity and the induction of organized vascular tissues. *Annals of botany*, 33(2):263–275, 1969.

[Sac72] T Sachs. A possible basis for apical organization in plants. *Journal of Theoretical Biology*, 37(2):353–361, November 1972.

[Sac00] T Sachs. Integrating cellular and organismic aspects of vascular differentiation. *Plant and cell physiology*, 41(6):649–656, 2000.

[SGH12] J Sun, J M Garibaldi, and C Hodgman. Parameter estimation using meta-heuristics in systems biology: a comprehensive review. *IEEE/ACM transactions on computational biology and bioinformatics / IEEE, ACM*, 9(1):185–202, January 2012.

[SGM+06] R S Smith, S Guyomarc'h, T Mandel, D Reinhardt, C Kuhlemeier, and Przemyslaw Prusinkiewicz. A plausible model of phyllotaxis. *Proceedings of the National Academy of Sciences*, 103(5):1301–1306, January 2006.

[SLC+08] Szymon Stoma, Mikael Lucas, Jérôme Chopard, Marianne Schaedel, Jan Traas, and Christophe Godin. Flux-based transport enhancement as a plausible unifying mechanism for auxin transport in meristem development. *PLoS computational biology*, 4(10):e1000207–, 2008.

[SLH+00] H Schoof, M Lenhard, A Haecker, K F Mayer, G J u rgens, and T Laux. The stem cell population of Arabidopsis shoot meristems in maintained by a regulatory loop between the CLAVATA and WUSCHEL genes. *Cell*, 100(6):635–644, March 2000.

[SMFB06] E Scarpella, D Marcos, J Friml, and T Berleth. Control of leaf vascular patterning by polar auxin transport. *Genes & development*, 20(8):1015–1027, April 2006.

[SSJ09] Patrik Sahlin, Bo Söderberg, and Henrik Jönsson. Regulated transport as a mechanism for pattern generation: Capabilities for phyllotaxis and beyond. *Journal of Theoretical Biology*, 258(1):60–70, May 2009.

[vBdBStT13] K van Berkel, R J de Boer, B Scheres, and K ten Tusscher. Polar auxin transport: models and mechanisms. *Development*, 140(11):2253–2268, May 2013.

[VBF+11] Teva Vernoux, Géraldine Brunoud, Etienne Farcot, Valérie Morin, Hilde Van den Daele, Jonathan Legrand, Marina Oliva, Pradeep Das, Antoine Larrieu, Darren Wells, Yann Guédon, Lynne Armitage, Franck Picard, Soazig Guyomarc'h, Coralie Cellier, Geraint Parry, Rachil Koumproglou, John H Doonan, Mark Estelle, Christophe Godin, Stefan Kepinski, Malcolm Bennett, Lieven De Veylder, and Jan Traas. The auxin signalling network translates dynamic input into robust patterning at the shoot apex. *Molecular systems biology*, 7(1):508, 2011.

[vMvDdG+10] S van Mourik, A van Dijk, M de Gee, R Immink, K Kaufmann, G Angenent, R van Ham, and J Molenaar. Continuous-time modeling of cell fate determination in Arabidopsis flowers. *BMC Systems Biology*, 4(1):101–101, 2010.

[WABBe+11] C M Winter, R S Austin, S Blanvillain-Baufum e, M A Reback, M Monniaux, M F Wu, Y Sang, A Yamaguchi, N Yamaguchi, J E Parker, F Parcy, S T Jensen, H Li, and D Wagner. LEAFY target genes reveal floral regulatory logic, cis motifs, and a link to biotic stimulus response. *Developmental Cell*, 20(4):430–443, April 2011.

[WAS+92] D Weigel, J Alvarez, D R Smyth, M F Yanofsky, and E M Meyerowitz. LEAFY controls floral meristem identity in Arabidopsis. *Cell*, 69(5):843–859, May 1992.

[WFTG13] Michael Luke Walker, Etienne Farcot, Jan Traas, and Christophe Godin. The Flux-Based PIN Allocation Mechanism Can Generate Either Canalyzed or Diffuse Distribution Patterns Depending on Geometry and Boundary Conditions. *PloS one*, 8(1):e54802, January 2013.

[WKVB+10] Krzysztof Wabnik, J u rgen Kleine-Vehn, Jozef Balla, Michael Sauer, Satoshi Naramoto, Vil e m Rein o hl, Roeland M H Merks, Willy Govaerts, and Ji i Friml. Emergence of tissue polarization from synergy of intracellular and extracellular auxin signaling. *Molecular systems biology*, 6:447, December 2010.

[YTR10] R K Yadav, M Tavakkoli, and G V Reddy. WUSCHEL mediates stem cell homeostasis by regulating stem cell number and patterns of cell division and differentiation of stem cell progenitors. *Development*, 137(21):3581–3589, November 2010.

[YWW+13] N Yamaguchi, M F Wu, C M Winter, M C Berns, S Nole-Wilson, A Yamaguchi, G Coupland, B A Krizek, and D Wagner. A molecular framework for auxin-mediated initiation of flower primordia. *Developmental Cell*, 24(3):271–282, February 2013.